ELSEVIER

Journal of Structural Geology 30 (2008) 739–745

JOURNAL OF STRUCTURAL GEOLOGY

www.elsevier.com/locate/jsg

Feasibility of graphic determination of stress from fault/slip data

Yehua Shan*, Zian Li

Laboratory of Marginal Sea Geology, Guangzhou Institute of Geochemistry, Chinese Academy of Sciences, Guangzhou City 510640, PR China

Received 1 March 2007; received in revised form 5 November 2007; accepted 13 November 2007
Available online 17 November 2007

Abstract

The equation describing 2D sections through an ellipsoid is similar in formulation to the equation describing fault/slip directions in relation to the stress tensor, thus enabling the conversion between them. So, the existing graphic method for determining the optical indicatrix or fabric ellipsoid can be used to infer stress from fault/slip data if they are converted to sectional measurements. After conversion, fault/slip data are displayed on a stereogram, and then are directly used to determine the poles to the circular sections of the stress ellipsoid, from which the ellipsoid is readily reconstructed. This is of importance for visual appreciation in stress inversion. However, the graphic method is only applicable to cozonal sectional measurements, and is unable to discriminate spurious data. In order to make up for this deficiency, a computer-aided method has been developed in this paper, and its feasibility illustrated by using an example.

Keywords: Fault/slip data; Section measurements of stretching lineation; Strain ellipse; Conversion; Stress; Fresnel's theorem

1. Introduction

In stress inversion using striated faults, fault/slip data measured at outcrop are used to infer the palaeostress that produced or reactivated the faults observed. Both the principal directions and the stress ratio are obtained in this way, thus rendering it the most complete stress gauge among structural analysis techniques (Ramsay and Lisle, 2000). Conventionally, only single-phase fault/slip data are used, as required by the assumption of a homogeneous palaeostress field. This applicability is very limited, because the collected data are commonly polyphase, due to variability of the tectonic stress field through geologic time. A recent approach (Blenkinsop et al., 2006) is to extend this conventional technique to polyphase fault/slip data in a variety of ways. The difficulty in such extension is the nonlinearity of the inversion and the dimensionality of the parameter space. The nonlinearity may be reduced to a great deal by adopting Fry's (1999) transformation to six dimensional parameter space, in which single-phase fault/slip data tend to be distributed in a hyperplane to which the solution of stress is normal. The inversion is hence simplified to look for all such hyperplanes among the datum vectors, each of which encapsulates both fault orientation and slip orientation (Shan et al., 2003). However, in the case of polyphase data, there generally exist many local minima in the parameter space that would prevent most existing stress inversion algorithms that proceed by minimizing their peculiar objective functions from reaching the global minimum (Shan et al., 2008b). This issue is further aggravated by the rather large dimension of the parameter space.

Recently, Shan et al. (2008a) deduced a simple linear equation for sectional measurements of stretching lineation. They assumed that stretching lineation is coincident with the long axis of a fabric ellipse, and that the fabric ellipsoid is identical to the strain ellipsoid. On that basis, they solved the equation, under an auxiliary constraint, for the relative strain ellipsoid. They noticed the similarity in formulation between strain inversion and stress inversion. Accordingly, it seems theoretically possible to transform fault/slip data and sectional measurements of stretching lineation to each other in some way.

It is confirmed by this short communication that there exists such a transformation between the two kinds of data. This

* Corresponding author. Tel.: +86 20 85290763; fax: +86 20 85290130.
E-mail address: shanyehua@yahoo.com.cn (Y. Shan).

0191-8141/$ - see front matter © 2007 Elsevier Ltd. All rights reserved.
doi:10.1016/j.jsg.2007.11.005

enables use of the graphic method for determining strain ellipsoid from sectional measurements (Lisle, 1976) to invert stress from fault/slip data. In this way, fault/slip data after conversion can be displayed on a stereogram, familiar to any structural geologist. They are directly used to determine the poles to the circular sections of the stress ellipsoid, from which the stress ellipsoid/tensor can be restored. Visual appreciation of the homogeneity or single-phase nature of a given data set is therefore readily achieved.

A similar idea for unifying the stress and the strain construction methods can be found in the papers of Fry (1992), Lisle (1998) and others (see their cited authors) who adapted the graphic methods, that they had used for deriving the direction of shear stress, so as to determine analogously the direction of finite shear strain. But all this work is based upon the knowledge of the stress or the strain, in the opposite direction to the goal of this study.

2. Theory

In this section, we will introduce the recent study of Shan et al. (2008a,b), and encourage interested readers to refer to their papers for more detailed explanation.

Conventionally, a strain ellipsoid is defined as a quadric surface centered at the origin in the Cartesian system (Fig. 1). It is described by the following equation: (e.g., Owens, 1984; Robin, 2002; Shan et al., 2008b)

$$\begin{bmatrix} x & y & z \end{bmatrix} \begin{bmatrix} b_{11} & b_{12} & b_{13} \\ b_{21} & b_{22} & b_{23} \\ b_{31} & b_{32} & b_{33} \end{bmatrix} \begin{bmatrix} x \\ y \\ z \end{bmatrix} = 1 \tag{1}$$

where x, y and z are the coordinates of a point on the ellipsoid in terms of the X-, Y- and Z-axis, respectively, and b_{ij} (i, $j = 1, 2, 3$) is an element of the shape matrix. As the shape matrix is symmetrical, we need to determine only six unknown independent elements, b_{ij} (i, $j = 1, 2, 3$; $i \geq j$). The determination may be made in many ways, on the basis of various types of sectional measurements of the strain ellipses observed on planar sections through the strain ellipsoid (Shan et al., 2008b).

In this paper we are only interested in the direction of the long axis of the elliptical section. Measurements required are the dip direction (α) and dip angle (β) of the section plane, and the pitch (θ) of the long axis of the sectional ellipse of the 3-D ellipsoid. The pitch is defined as the angle between the long axis of the strain ellipse and the westwards or eastwards strike of the plane dipping towards the south or north (Fig. 1).

A simple expression of the strain ellipse on the plane can be obtained through a series of rotations that transform the plane into a horizontal one where the long axis of the strain ellipse is aligned with the X-axis. This manipulation can be implemented by rotating around the Z-axis with an angle of $-\alpha$, around the Y-axis with an angle of $-\beta$, and finally around the Z-axis with an angle of $\theta - 90^\circ$. Let T stand for the inverse manipulation of these rotations that defines the relationship between the old and the new coordinate systems:

$$\begin{bmatrix} x \\ y \\ z \end{bmatrix} = T \begin{bmatrix} x' \\ y' \\ z' \end{bmatrix} = \begin{bmatrix} t_{11} & t_{12} & t_{13} \\ t_{21} & t_{22} & t_{23} \\ t_{31} & t_{32} & t_{33} \end{bmatrix} \begin{bmatrix} x' \\ y' \\ z' \end{bmatrix} \tag{2}$$

$$T = \begin{bmatrix} \cos\alpha & -\sin\alpha & 0 \\ \sin\alpha & \cos\alpha & 0 \\ 0 & 0 & 1 \end{bmatrix} \begin{bmatrix} \cos\beta & 0 & -\sin\beta \\ 0 & 1 & 0 \\ \sin\beta & 0 & \cos\beta \end{bmatrix} \times \begin{bmatrix} \cos(90^\circ - \theta) & \sin(90^\circ - \theta) & 0 \\ -\sin(90^\circ - \theta) & \cos(90^\circ - \theta) & 0 \\ 0 & 0 & 1 \end{bmatrix} \tag{3}$$

Applying this transformation to Eq. (1) and letting $z' = 0$ leads to the expression of the strain ellipse in the new coordinate system as follows:

$$\begin{bmatrix} x' & y' \end{bmatrix} \begin{bmatrix} t_{11}t_{11}b_{11} + 2t_{11}t_{21}b_{12} + 2t_{11}t_{31}b_{13} + t_{21}t_{21}b_{22} + 2t_{21}t_{31}b_{23} + t_{31}t_{31}b_{33} & t_{11}t_{12}b_{11} + (t_{11}t_{22} + t_{21}t_{12})b_{12} + (t_{11}t_{32} + t_{31}t_{12})b_{13} + t_{21}t_{22}b_{22} + (t_{21}t_{32} + t_{31}t_{22})b_{23} + t_{31}t_{32}b_{33} \\ \text{(symmetrical)} & t_{12}t_{12}b_{11} + 2t_{12}t_{22}b_{12} + 2t_{12}t_{32}b_{13} + t_{22}t_{22}b_{22} + 2t_{22}t_{32}b_{23} + t_{32}t_{32}b_{33} \end{bmatrix} \begin{bmatrix} x' \\ y' \end{bmatrix} = k \tag{4}$$

where k is the scale parameter, which is different for each individual section of the strain ellipsoid.

The new coordinate system is specified as having the section ellipse symmetrical to its axes, so the matrix in Eq. (4) must have zero for its off-diagonal elements. Therefore, we have, specifying the off-diagonal elements, the following linear equation.

$$\begin{bmatrix} t_{11} & t_{21} & t_{31} \end{bmatrix} \begin{bmatrix} b_{11} & b_{12} & b_{13} \\ b_{21} & b_{22} & b_{23} \\ b_{31} & b_{32} & b_{33} \end{bmatrix} \begin{bmatrix} t_{12} \\ t_{22} \\ t_{32} \end{bmatrix} = 0 \tag{5}$$

By its definition, the matrix T is an orthogonal matrix, and, accordingly, it consists of orthogonal rows. Hence, $[t_{11}, t_{21}, t_{31}]$ and $[t_{12}, t_{22}, t_{32}]$, are perpendicular to each other. Eq. (5) constitutes the basis of Shan et al.'s (2008a) using this kind of sectional measurement to determine the relative strain ellipsoid in a rock.

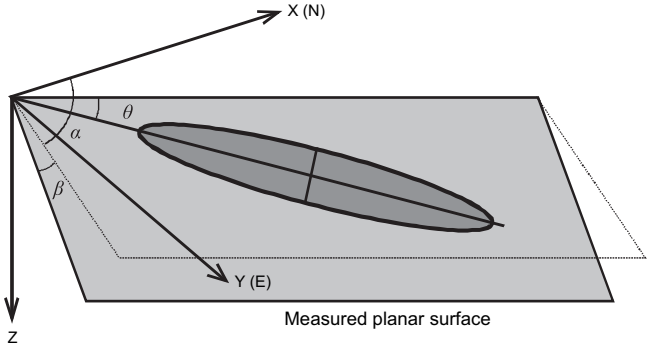

Fig. 1. Elements of strain measurement made on the planar surface in the Cartesian coordinate system where the X-axis is directed towards the north, the Y-axis towards the east, and the Z-axis upwards (Shan et al., 2008a). The blank rectangle, marked by three dashed lines and one thick line, represents a part of the horizontal (X–Y) plane. The gray rectangle marked by thick lines represents the plane where the strain ellipse is measured. See the text and Table 1 for symbol definitions.

On the other hand, it is assumed in stress inversion that there is parallelism between the maximum shear traction on the fault plane and the slip line. This important assumption, although it remains in dispute for reactivated faults (Pollard and Rubin, 1993; Nieto-Samaniego, 1999), leads to the following basic equation (see Angelier, 1979; Shan et al., 2003).

$$\begin{bmatrix} n_1 & n_2 & n_3 \end{bmatrix} \begin{bmatrix} \sigma_{11} & \sigma_{12} & \sigma_{13} \\ \sigma_{21} & \sigma_{22} & \sigma_{23} \\ \sigma_{31} & \sigma_{32} & \sigma_{33} \end{bmatrix} \begin{bmatrix} l_1 \\ l_2 \\ l_3 \end{bmatrix} = 0 \tag{6}$$

where n_i ($i = 1, 2, 3$) is an element of the normal vector to the fault plane, l_i ($i = 1, 2, 3$) is an element of the unit vector on the fault plane and perpendicular to the slip line, and σ_{ij} ($i, j = 1, 2, 3$) is an element of the unknown stress tensor. The vectors n and l are perpendicular to each other, and $\sigma_{ij} = \sigma_{ji}$.

There is no difference in formulation between Eqs. (5) and (6), suggesting equivalence between the shape matrix and the stress tensor, in some sense. This enables us to convert the two types of data, sectional measurements of stretching lineations and fault/slip data, to each other in a way that leads to no difference in magnitude between the estimated shape matrix and the estimated stress tensor. Such conversion is justified by the fact that both the estimate of strain and the estimate of stress are relative in magnitude. Sectional measurements of the strain ellipse are only used to determine the relative strain ellipsoid (Shan et al., 2008a), and fault/slip data to determine the relative stress tensor (Fry, 1999; Shan et al., 2003).

In a way similar to that in Eqs. (2) and (3), we define from Eq. (6) an orthogonal transformation matrix T' as follows.

$$T' = \begin{bmatrix} l_1 & n_1 & s_1 \\ l_2 & n_2 & s_2 \\ l_3 & n_3 & s_3 \end{bmatrix} \tag{7}$$

where s_i ($i = 1, 2, 3$) is an element of the slip line on the fault plane.

Table 1
A set of four fabric measurements from Lisle (1976) (see his third example) and its converted fault/slip data

Sectional measurements (°)				Converted fault/slip data (°)			
Exposure planes		Fabric traces		Fault planes		Slip lines	
Dip direction	Dip angle	Bearing	Plunge	Dip direction	Dip angle	Bearing	Plunge
133	90	223	40	43	50	313	0
35	90	305	47	125	43	35	0
90	90	180	9	0	81	270	0
181	90	271	64	91	26	1	0

As is thereby required, $T = T'$. According to this equation, we calculate from fault/slip data their counterparts in the format of section measurements of strain ellipse, or from sectional measurements of strain ellipse their counterparts in the format of fault/slip data. For example, the converted fault/slip data listed in Table 1 are calculated in the way described above from the third fabric example of Lisle (1976).

Nevertheless, for either a sectional measurement or a fault/slip datum, we may have more than one counterpart of it because there are many ways to define the orthogonal matrix T'. Each of these counterparts gives rise to similar estimate of strain or of stress.

3. Graphic determination

In the way described above, a set of measured fault/slip data may be converted into sectional measurements of strain ellipse. Such sectional measurements are solved for the relative strain ellipsoid that, theoretically speaking, has no difference in magnitude from the relative stress tensor directly obtained from the

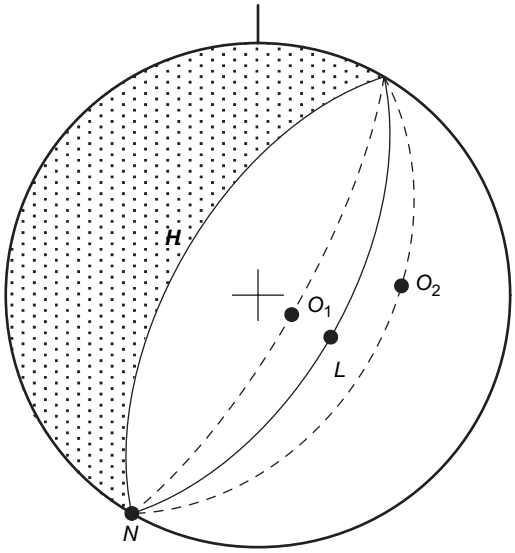

Fig. 2. An illustration of Fresnel's theorem on a stereogram. A section plane has a normal (N) and a fabric trace (L). O_1 and O_2 are poles to circular sections of the fabric ellipsoid. The $\angle O_1NO_2$ is bisected by the plane containing N and L. The plane $\boldsymbol{H}$ is symmetrical about a vertical plane along strike to the plane NL. Dotted region bounded by $\boldsymbol{H}$ can be eliminated because it does not contain the two poles.

fault/slip data themselves. This is an important conclusion drawn in this paper. This makes it possible to use some ways peculiar to sectional measurements of strain ellipse (e.g., Lisle, 1976) to determine the stress recorded by fault/slip data.

The idea of graphic determination can be derived from Tocher (1964) and others, who used a minimal number of four independent cozonal extinction measurements to determine stereographically the three axes of the optic indicatrix. It was later applied to fabric analysis by Lisle (1976). It is worthwhile to note that there is no essential difference in formulating sectional measurements among the optic indicatrix, the fabric ellipsoid and the strain ellipsoid. The determination was based upon Fresnel's theorem in optical crystallography. In the theorem (see Tocher, 1964; Lisle, 1976), plane NL that contains the normal N to the section plane and the elimination/trace/lineation on the plane (L) bisects the angle between planes NO_1 and NO_2, namely, $\angle LNO_1 = \angle LNO_2$, where O_1 and O_2 are the poles to the circular sections in the optical indicatrix/fabric ellipsoid/strain ellipsoid (Fig. 2).

Tocher (1964) developed for this purpose the progressive elimination method, which is readily realized by hand using a stereonet. Subsequently, Lisle (1976) used it to determine the fabric ellipsoid in a rock. The following introduction to the method is based upon fabric analysis. First of all, one needs to distinguish whether the distribution of the fabric traces is equatorial or polar, by inspecting their plots on the stereogram, and then replace only the fabric traces in the equatorial distribution by vectors that are perpendicular to them on the section planes.

Let us draw a plane $\boldsymbol{H}$, symmetrical to the plane (NL) about a vertical plane containing the strike (Fig. 2), such that the two planes, $\boldsymbol{H}$ and NL, dip towards each other, and have the same dip angle. In the light of Fresnel's theorem, the two poles to the circular sections, O_1 and O_2, do not locate in the dotted region bounded by plane $\boldsymbol{H}$ and the horizon. Therefore, the dotted region can be eliminated from the vector space in which to search for the poles. With increase of measurements taken into account, the vector space is more greatly reduced in this way. However, the reduction from this simple elimination will eventually lead to one or more relatively wide acceptable regions, within which we cannot determine the loci of O_1 and O_2 to a satisfactory degree. As a remedy, some accommodation constraints by these measurement themselves must be added during the progressive elimination to reduce the accepted region further. Including more measurements generally leads to better determination of the loci, but makes the process much more complicated and time-consuming.

Once the loci of O_1 and O_2 are determined in the way described above, they are used together with the fault slip sense to calculate the three strain principal directions and their relative magnitudes (Lisle, 1976). The intermediate principal direction is normal to the great circle through O_1 and O_2, which are bisected by both the maximum and the minimum principal directions. Stress ratio can be calculated from the angle between the two loci. However, there exist two options for locating the maximum or the minimum principal direction, and for defining the angle in the above equation as either acute or obtuse, mutually complementary. Resolving these options requires the knowledge of the fault slip senses.

4. Computer-aided display

Sectional measurements converted in the above-mentioned way from fault/slip data are generally not cozonal and vertically dipping. This brings difficulty in the direct application of the progressive elimination method (Tocher, 1964), which primarily deals with cozonal sectional measurements. For each sectional measurement not of vertical dip, we need to rotate the section plane to dip vertically, and then reduce the accepted region in the vector space, and finally retro-rotate both the rotated plane and the accepted region to the initial

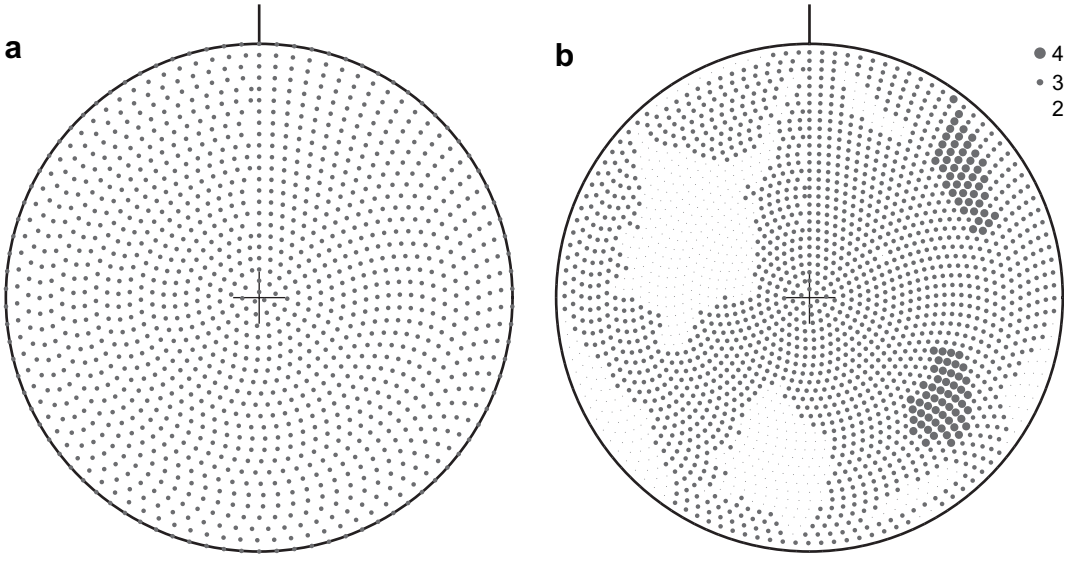

Fig. 3. For an angular width of 3°, stereograms showing (a) the mesh of the vector space, and (b) the result of applying the method proposed in this paper to the third example of Lisle (1976). The four-data example is listed in Table 1. Lower hemisphere and equal-area projection. Northwards is towards the top of the page.

Table 2
A set of 10 fault/slip data from Shan et al. (2003) (see the first 10 data of the first subset in their appendix) and their converted fault/slip data

Fault/slip data (°)				Converted sectional measurements (°)			
Fault planes		Slip lines		Section planes		Lineations	
Dip direction	Dip angle	Bearing	Plunge	Dip direction	Dip angle	Bearing	Plunge
0.01	4.88	352.62	4.84	172.62	85.16	180.01	85.12
216.49	63.08	163.70	49.98	343.70	40.02	36.49	26.92
348.46	10.93	353.22	10.90	173.22	79.10	168.46	79.06
185.39	23.45	191.65	23.33	11.65	66.67	5.39	66.55
94.65	48.03	57.63	41.60	237.63	48.40	274.64	41.97
32.24	34.08	354.25	28.07	174.25	61.93	212.24	55.92
209.60	54.05	177.22	49.35	357.22	40.65	29.60	35.95
213.09	30.78	202.06	30.31	22.06	59.69	33.09	59.22
315.59	84.32	226.99	13.77	46.99	76.23	135.59	5.68
261.44	75.15	190.82	51.39	10.82	38.61	81.43	14.85

state. It is very time-consuming to carry out this process by hand, and very vulnerable to careless mistakes.

In addition, Tocher's (1964) method is most likely to fail in searching for the loci of O_1 and O_2, if there exist a few spurious data, because the method itself cannot discriminate spurious data from the entire set. It is, however, sometimes possible to solve this problem by careful inspection of each datum on a stereogram, but doing so takes much more time and energy.

For these reasons, we developed in this paper a computer-aided method for the same purpose, in which a grid search is used to look for the loci of the poles that account for the largest number of data. The procedure of this new method is described as follows:

(1) evenly mesh the vector space for a certain angular width, 3° in Fig. 3a, for instance, from which the best pair of poles, O_1 and O_2 will be looked for in the following steps,
(2) for each node of the mesh, look by grid search for another node that under a certain angular limit (in this paper, the same value as the angular width) can account for the largest number of sectional measurements when the two nodes are considered as the poles to the section ellipses, and mark the locus of each node on the stereogram with this number,
(3) look for the nodes having the maximum marked number,
(4) accept the pairs of nodes that account for the same data as the best solutions of the poles; otherwise, carefully inspect and delete the spurious data, and return to step 2,
(5) calculate the mean locus of accepted poles in a region, and
(6) for converted data, restore from the known pair of poles two possible solutions of the relative strain/stress tensor, principal directions and their relative magnitudes, and use the observed slip senses/lineations to determine the real solution; or for primary sectional measurements, just restore the strain principal directions and their relative magnitudes from the known pole pair.

Fig. 3b shows the result of applying our new method to the third example (Table 1) of Lisle (1976). Regions of a number of four fit data in each node are closely coincident with the eventually accepted regions by the elimination method (see Fig. 5 of Lisle, 1976). For the sake of graphical display on the stereogram, we used an angular width of 3° for this example, although a finer mesh will lead to a much closer match between them.

5. Application

The first 10 artificial fault/slip data (Table 2) of the first single-phase subset from Shan et al. (2003) (see their appendix) are taken in this section and used as an example. Applying the proposed method to them gives rise to the results shown in Fig. 4 and listed in Tables 2 and 3. For an

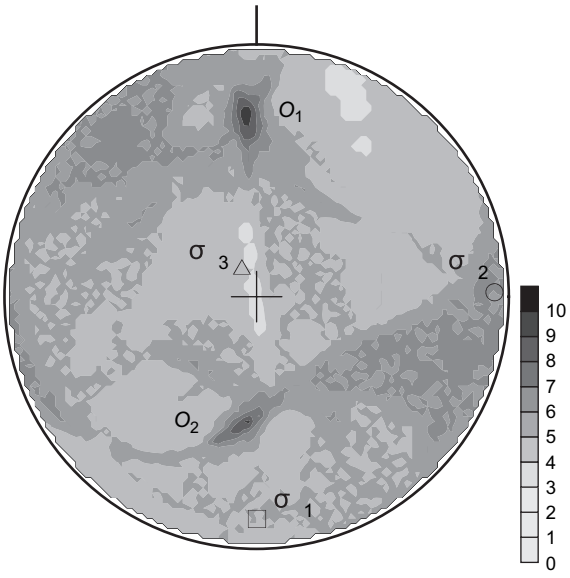

Fig. 4. Result on a stereogram of applying the proposed method to the first 10 data (Table 2) of the first single-phase subset from Shan et al. (2003) (see their appendix), using an angular width of 2°. Contours were drawn by using an interpolation of natural neighborhood. O_1 and O_2 are poles to circular sections of the stress ellipsoid. The calculated principal stress directions are shown by a square (σ_1), circle (σ_2) and triangle (σ_3). Lower hemisphere and equal-area projection. Northwards is towards the top of the page.

Table 3
Comparison between the prescribed and the determined stress tensors from the example listed in Table 2

	Stress principal directions (°)						Stress ratio
	Maximum		Intermediate		Minimum		
	Bearing	Plunge	Bearing	Plunge	Bearing	Plunge	
Prescribed	180.00	10.00	89.00	5.65	329.93	78.48	0.667
Estimated	179.91	10.69	88.94	5.12	333.73	78.12	0.663

assigned angular width of 2°, only three nodes of the mesh can account for all 10 data, and hence the loci of the two poles to circular sections are well determined (Fig. 4). This is simply ascribed to there being no inclusion of measurement errors in producing the artificial data under a certain prescribed stress. There is almost no difference between the prescribed and the determined stress tensors (Table 3), thus demonstrating the feasibility of the method developed in this paper.

6. Conclusions and remarks

There is no difference in formulation between equations describing sectional measurements of strain ellipse and fault/slip data, or Eqs. (5) and (6). This makes it possible to convert between the one kind and the other. Therefore, we can use the graphic method that has been proposed for determining the optical indicatrix or the fabric ellipsoid (Tocher, 1964; Lisle, 1976) to infer stress from fault/slip data if they are converted in some way to sectional measurements. Making this determination using a stereonet by hand is a little cumbersome but exciting.

However, Tocher's (1964) method is based just upon cozonal sectional measurements, and is unable to discriminate spurious data, if there are any, from the entire set. These would prohibit application of the graphic method to any set of converted fault/slip data that are generally not cozonal and that probably contain some spurious data. A computer-aided method has been developed in this paper to make up for this deficiency. It uses a grid search to look for the accepted regions of the poles to circular sections of the strain ellipsoid. A well-controlled example was taken to show the applicability and the feasibility of this new method.

After the conversion, fault/slip data can be displayed on a stereogram – a method familiar to all structural geologists – to determine the poles of circular sections of the stress ellipsoid. We can visualize what we do in this way. This is of importance in stress inversion, because nearly all existing algorithms proceed either in hyperspace (for example, Fry's, 1999 sigma space has a dimension of six) or by procedures in which the dimensionality of the problem is opaque. Visual appreciation is thus readily made to appraise the homogeneity of a given data set. It can be used to separate polyphase fault/slip data into many single-phase subsets, instead of adopting some stopping rule. We believe that this will open a new direction for palaeostress analysis.

Acknowledgement

This work is funded by National Basic Research Program of China 973 (Grant 2007CB411307), Hundred Talent Program of Chinese Academy of Sciences (KZCX 0543081001), and National Natural Science Foundation of China (Grant 40672144). We are greatly indebted to Norman Fry who checked the written English of this article and made numerous modifications to it, and two reviewers, Tom Blenkinsop and Richard J. Lisle who made valuable suggestions about it.

Appendix

A list of symbols and their definitions

Symbols	Definitions	Comments
x, y, and z	Coordinates of a point on the ellipsoid in the real state.	Eqs. (1) and (2).
x', y', and z'	Coordinates of a point on the ellipsoid in the rotated (reference) state.	Eqs. (2) and (4).
b_{ij}	Elements of a shape matrix.	$i, j = 1, 2, 3$; Eqs. (1), (4) and (5).
ε_1, ε_2, and ε_3	Magnitudes of the principal axes of an ellipsoid.	$\varepsilon_1 \geq \varepsilon_2 \geq \varepsilon_3 > 0$
α and β	Dip direction (azimuth) and dip angle of a certain measured planar surface.	Eq. (3) and Fig. 1.
θ	Pitch of the long axis of a strain ellipse on the planar surface.	Eq. (3) and Fig. 1.
T	Inverse rotation matrix	Eqs. (2) and (3).
t_{ij}	Elements of inverse rotation matrix.	$i, j = 1, 2, 3$; Eqs. (2), (4) and (5).
k	Elliptical parameter.	Eq. (4).
σ_{ij}	Elements of a stress tensor.	$i, j = 1, 2, 3$; Eq. (6).
σ_i	Principal stress directions.	$i = 1, 2, 3$.
n_i	Elements of the normal to a fault plane.	$i = 1, 2, 3$; Eqs. (6) and (7).
l_i	Elements of the unit vector on a fault plane that is perpendicular to the slip line.	$i = 1, 2, 3$; Eqs. (6) and (7).
s_i	Element of the slip line on a fault plane	$i = 1, 2, 3$; Eq. (7).
T'	Transformation matrix.	Eq. (7).
O_i	Pole to circular section of an ellipsoid.	$i = 1, 2$; Figs. 2 and 4.
N	Normal to a section plane.	Fig. 2
L	Fabric trace or lineation on a section plane.	Fig. 2
NL	Plane containing N and L.	Fig. 2
$\boldsymbol{H}$	Plane symmetrical, about a vertical plane along the strike, to the plane NL.	Fig. 2

References

Angelier, J., 1979. Determination of the mean principal directions of stresses for a given fault population. Tectonophysics 56, T17–T26.

Blenkinsop, T., Lisle, R., Ferrill, D., 2006. Introduction to the Special Issue on New Dynamics in Palaeostress Analysis. Journal Structural Geology 28, 941–942.

Fry, N., 1992. Direction of shear. Journal of Structural Geology 14, 253–255.

Fry, N., 1999. Striated faults: visual appreciation of their constraint on possible palaeostress tensors. Journal of Structural Geology 21, 7–22.

Lisle, R.J., 1976. Some macroscopic methods of fabric analysis. Journal of Geology 84, 225–235.

Lisle, R.J., 1998. Simple graphical construction for the direction of shear. Journal of Structural Geology 20, 969–973.

Nieto-Samaniego, A.F., 1999. Stress, strain and fault patterns. Journal of Structural Geology 21, 1065–1070.

Owens, W.H., 1984. The calculation of a best-fit ellipsoid from elliptical sections on arbitrarily orientated planes. Journal of Structural Geology 6, 571–578.

Pollard, D.D., Rubin, S.M., 1993. Stress inversion methods: are they based on faulty assumptions? Journal of Structural Geology 15, 1045–1054.

Ramsay, J.G., Lisle, R.J., 2000. The Techniques of Modern Structural Geology: Volume 3: Applications of Continuum Mechanics in Structural Geology. Academic Press, London.

Robin, P.-Y.F., 2002. Determination of fabric and strain ellipsoids from measured sectional ellipses - theory. Journal of Structural Geology 24, 531–544.

Shan, Y., Suen, H., Lin, G., 2003. Separation of polyphase fault/slip data: an objective-function algorithm based on hard division. Journal of Structural Geology 25, 829–840.

Shan, Y., Gong, F., Li, Z., Lin, G., 2008a. Determination of relative strain ellipsoids from sectional measurements of stretch lineation. Journal of Structural Geology 30, 682–686.

Shan, Y., Liu, L., Peng, S., 2008b. An analytical approach for determining strain ellipsoids from measurements on planar surfaces. Journal of Structural Geology 30, 539–546.

Tocher, F.E., 1964. Direct stereographic determination of the optic axes from a few extinction measurements: a progressive elimination technique. Mineralogy Magazine 33, 780–789.